The inhibition of LSD1 via sequestration contributes to tau-mediated neurodegeneration

Amanda K. Engstrom[1], Alicia C. Walker[1], Rohitha A. Moudgal[1], Dexter A. Myrick[1], Stephanie M. Kyle[1], Yu Bai,[1] M Jordan Rowley[2], David J. Katz[1*]

[1] Department of Cell Biology, Emory University School of Medicine, Atlanta GA 30322, USA.
[2] Department of Genetics, Cell Biology, and Anatomy, University of Nebraska Medical Center, Omaha, NE 68198

*Correspondence to: David J

Email: djkatz@Emory.edu.

Classification

Biological Sciences: Neuroscience

Keywords

LSD1, Neurodegeneration, Tauopathy, Alzheimer's disease

Author Contributions

A.K.E and D.J.K. conceived and designed the study and wrote the manuscript. A.K.E. performed experiments with the help of A.C.W, S.M.K, R.A.M and Y.U under the direction of D.J.K. D.A.M and M.J.R performed bioinformatics analysis on the RNA sequencing data. A.K.E, A.C.W, S.M.K, and R.A.M analyzed all other data and interpreted results. All authors discussed the results and commented on the manuscript.

This PDF file includes:

Main Text

Main Figures 1-6

ABSTRACT

Tauopathies are a class of neurodegenerative diseases associated with pathological tau. Despite many advances in our understanding of these diseases, the direct mechanism through which tau contributes to neurodegeneration remains poorly understood. Previously, our lab implicated the histone demethylase LSD1 in tau-induced neurodegeneration by showing that LSD1 localizes to pathological tau aggregates in Alzheimer's disease cases, and that it is continuously required for the survival of hippocampal and cortical neurons in mice. Here, we utilize the P301S tauopathy mouse model to demonstrate that pathological tau can exclude LSD1 from the nucleus in neurons. In addition, we show that reducing LSD1 in these mice is sufficient to highly exacerbate tau-mediated neurodegeneration and tau-induced gene expression changes. Finally, we find that overexpressing LSD1 in the hippocampus of tauopathy mice, even after pathology has formed, is sufficient to significantly delay neurodegeneration and counteract tau-induced expression changes. These results suggest that inhibiting LSD1 via sequestration contributes to tau-mediated neurodegeneration. Thus, LSD1 is a promising therapeutic target for tauopathies such as Alzheimer's disease.

SIGNIFICANCE STATEMENT

We have made the novel discovery that pathological tau functions through the histone demethylase LSD1 in the Alzheimer’s disease pathway. Thus, we have identified a mechanism that links tau to the downstream neuronal dysfunction pathways. This step can potentially be targeted therapeutically, after the onset of dementia symptoms, to block the progression of dementia in Alzheimer’s disease patients.

54 **INTRODUCTION**

55 Tauopathies such as corticobasal degeneration, progressive supranuclear palsy, and
56 frontotemporal lobar degeneration with tau inclusions are neurodegenerative diseases
57 pathologically defined by different forms of tau positive intraneuronal deposits (*1-5*). In addition
58 to these primary tauopathies, neuropathological observations of postmortem Alzheimer's disease
59 (AD) brains show the presence neurofibrillary tangles (NFTs) of hyperphosphorylated tau
60 protein, as well as plaques containing β-amyloid (Aβ) peptide (*6-9*). AD is the leading cause of
61 age-related dementia, resulting from neuronal cell death in the frontal and temporal cortices, as
62 well as the hippocampus (*7*). As dementia progresses, the spatial pattern of tau pathology highly
63 correlates with the level of cognitive impairment (*10-13*). In addition, Aβ oligomers and/or
64 plaques can enhance tau pathology in various mouse models (*14, 15*), and there is increasing
65 evidence that accumulation of Aβ plaques can contribute to tau pathology (*3, 16, 17*). The most
66 well-defined physiological role of tau is in stabilizing microtubules, particularly in neuronal
67 axons (*2*). However, in the pathological state, tau becomes aberrantly phosphorylated (*2, 18, 19*),
68 truncated (*1, 4*), and aggregates into oligomers and larger insoluble filaments (*20, 21*). This
69 pathology is thought to trigger synaptic loss, dramatic genome-wide expression changes,
70 increased inflammatory response, and neuronal cell death (*22-25*). These data suggest that
71 pathological tau may be a downstream mediator of the neurotoxic effects leading to neuronal
72 degeneration in AD.

73 Previously, our lab demonstrated that deleting the histone demethylase *Lsd1* in adult mice
74 leads to significant neuronal cell death in the hippocampus and cortex with associated learning
75 and memory defects (*26*). In this mouse model, loss of *Lsd1* induces genome-wide expression
76 changes that significantly overlap with those observed in the brains of postmortem human AD

77 cases, but not other neurodegenerative diseases, such as Parkinson's disease or amyotrophic
78 lateral sclerosis (ALS) cases. Consistent with this overlap, we observed LSD1 protein
79 mislocalized to cytoplasmic NFTs, but not associated with Aβ plaques in AD cases or Lewy
80 bodies of α-synuclein in Parkinson's disease cases (*26*). In control cases, LSD1 remains strictly
81 confined to the nucleus (*26*), due to it's well-defined nuclear localization signal (*27*). These data
82 highlight the requirement for LSD1 in neuronal survival and suggest that the nuclear function of
83 the histone demethylase LSD1 could be disrupted by mislocalization to pathological tau.

84 To investigate how LSD1 may contribute to tau-mediated neurodegeneration, we utilized
85 the PS19 P301S tauopathy mouse model (hereafter referred to as PS19 Tau). PS19 Tau mice
86 express a P301S mutated form of the human tau protein, originally identified in a frontotemporal
87 dementia with parkinsonism (FTDP-17) patient, driven by the prion promoter throughout the
88 nervous system (*28*). When expressed in mice, the P301S tau protein is prone to
89 hyperphosphorylation and somatodendritic aggregation, without the presence of Aβ plaques.
90 PS19 Tau mice develop a heavy pathological tau burden and have been well characterized for the
91 temporal progression of tau pathology and disease-related phenotypes (*29, 30*). However, the
92 mechanism of neuronal cell death caused by pathological tau is still unknown.

93 Here, we provide functional data that the inhibition of LSD1 function contributes to tau
94 induced neurodegeneration. We demonstrate in PS19 Tau mice that pathological tau sequesters
95 LSD1 in the cytoplasm of neurons throughout the brain. This results in depletion of LSD1 from
96 the nucleus. Additionally, we provide genetic and molecular evidence that pathological tau
97 contributes to neurodegeneration by disrupting LSD1. Finally, we show that overexpressing
98 LSD1 in hippocampal neurons is sufficient to suppress neuronal cell death even after
99 pathological tau has formed. We propose that pathological tau contributes to neuronal cell death

100 by sequestering LSD1 in the cytoplasm, depleting the nuclear pool of LSD1 that is required for
101 neuronal survival.
102
103 **RESULTS**
104 **Tau pathology depletes LSD1 from the nucleus in the PS19 Tau mouse model**
105 Previously, we showed in human AD cases that LSD1 protein inappropriately colocalizes with
106 NFTs in the cell body of hippocampal and cortical neurons, while in unaffected controls LSD1
107 was properly localized exclusively to the nucleus (*26*). However, because neurons in AD cases
108 with intracellular NFTs presumably die and are cleared, it was difficult to determine whether tau
109 prevents LSD1 from localizing to the nucleus in a dying neuron. To address this possibility, we
110 performed LSD1 immunofluorescence on 12 month old PS19 Tau mice, which have significant
111 tau pathology (*28*). Because PS19 Tau mice undergo neurodegeneration over a shortened period,
112 there are more neurons undergoing neurodegeneration at any given time point. Thus, we
113 reasoned that it may be possible to observe LSD1 depletion from the nucleus. Similar to what we
114 observe in humans, LSD1 protein in 12 month old Wild Type mice was strictly localized to the
115 nucleus of neurons in the cerebral cortex (Fig. 1A-C) and the hippocampus (Fig. S1 A-C). This
116 was expected since LSD1 has a well-defined nuclear localization signal (*27*). However, in 12
117 month old PS19 Tau mice, LSD1 protein was sequestered in the cytoplasm and depleted from the
118 nucleus both in the cerebral cortex (Fig. 1D-F,M,N) and the hippocampus (Fig. S1 D-F). These
119 are both regions where we observe substantial cytoplasmic tau pathology (Fig. 1G-I; Fig. S1 G-
120 I). Similarly, in other brain regions that accumulate tau pathology, such as the thalamus and
121 amygdala, LSD1 was localized to the nucleus in 12 month old Wild Type control mice (Fig. S1
122 J-O), but abnormally localized to the cytoplasm in PS19 Tau mouse littermates (Fig. S1 P-U).

123 Overall, we observed sequestration of LSD1 in 6 out of 7 mice analyzed. In each of the 6 mice,
124 there were varying levels of sequestration ranging from LSD1 found in both the nucleus and
125 cytoplasm (Fig. S1 V-X, M,N), to depletion from the nucleus (Fig. S1 Y-DD, M,N). The mouse
126 that has little sequestration (denoted by the ^ in Fig. 1M) has extensive tau pathology, but this
127 pathology is largely extracellular rather than cytoplasmic, indicating that neurons with extensive
128 LSD1 sequestration may have died and been cleared.
129

130 **Reduction of LSD1 increases the mouse tauopathy phenotype**

131 If the presence of pathological tau in the cytoplasm is leading to neuronal cell death through the
132 sequestration and nuclear depletion of LSD1, we would expect that lowering the overall levels of
133 LSD1 would accelerate depletion and exacerbate the progression of disease. To test this, we
134 made PS19 Tau mice heterozygous for *Lsd1* (hereafter referred to as PS19;*Lsd1*$^{\Delta/+}$, Fig. S2 A).
135 *Lsd1* was deleted using *Vasa-Cre* (*31*). The *Lsd1* deletion created when the floxed allele
136 recombines is a null allele that has previously been characterized (*26, 32, 33*). Once the *Lsd1*
137 deletion passes through the germline, *Lsd1* is heterozygous throughout the mouse. These *Lsd1*
138 heterozygotes (hereafter referred to as *Lsd1*$^{\Delta/+}$) have a functioning copy of *Lsd1* and don't have
139 any phenotypes associated with the heterozygous loss of LSD1 function (*33-35*). Thus, *Lsd1*
140 heterozygosity does not completely compromise LSD1 function. Instead mice that are
141 heterozygous for *Lsd1* are sensitized to mechanisms affecting LSD1 localization and function.
142 Consistent with this, we observed a 20% reduction in transcript levels (Fig. S2 B) and a 35%
143 reduction in protein levels (Fig. S2 C,D) in *Lsd1*$^{\Delta/+}$ mice compared to their *Lsd1*$^{+/+}$ littermates.
144 Surprisingly, PS19 Tau mice have a 20% increase in LSD1 protein levels compared to *Lsd1*$^{+/+}$
145 littermates. It is possible that this is due to some type of compensation because LSD1 is being

146 sequestered. Nevertheless, consistent with the reduction in LSD1 that we observe in *Lsd1*$^{\Delta/+}$
147 mice, PS19;*Lsd1*$^{\Delta/+}$ mice have a similar 14% reduction in transcript levels (Fig. S2 B) and a 31%
148 reduction in protein levels (Fig. S2 C,D) compared to PS19 Tau littermates. This enables us to
149 directly assess the effect of reducing LSD1 on tau-induced neurodegeneration. In addition, all
150 genotypes were born at normal Mendelian ratios with equal male/female ratios.

151 To determine if reducing LSD1 protein levels accelerates tau-induced depletion of LSD1
152 from the nucleus, we analyzed localization of LSD1 in PS19;*Lsd1*$^{\Delta/+}$ mice versus PS19 Tau
153 controls. When one copy of *Lsd1* was removed from PS19 Tau mice, there was a significant
154 decrease in the nuclear localization of LSD1 compared to PS19 Tau mice (Fig. 1J-N),
155 accompanied by an increase in the number of cells that have LSD1 in both the nucleus and the
156 cytoplasm (Fig 1J-N). This suggests that reducing LSD1 enables tau to accelerate the depletion
157 of LSD1.

158 Since lowering LSD1 accelerates tau-induced depletion of LSD1 from the nucleus, we
159 determined if this acceleration exacerbates the progression of disease, by analyzing survival,
160 paralysis, neurodegeneration and genome-wide gene expression changes in PS19;*Lsd1*$^{\Delta/+}$ mice
161 versus PS19 Tau controls. As expected, *Lsd1*$^{\Delta/+}$ mice had normal survival (Fig. 2A). In contrast,
162 PS19 Tau mice had a reduced overall survival (Fig. 2A) (*28*). When one copy of *Lsd1* was
163 removed from PS19 Tau mice, their reduced survival was significantly exacerbated (P-value =
164 0.0017, Fig. 2A). As expected, there was little effect on the onset of reduced viability. The initial
165 decline in the survival of PS19;*Lsd1*$^{\Delta/+}$ mice started only slightly earlier than PS19 Tau mice, but
166 after the appearance of hyperphosphorylated (AT8 positive) pathological tau in neurons, as
167 quantified by the average AT8 positive tau immunoreactivity per area in the hippocampus and
168 cortex (Fig. S6 K-M)(*28*). This suggests that pathological tau may have to be present in order for

169 *Lsd1* heterozygosity to have deleterious effects. Subsequently, PS19;*Lsd1*$^{\Delta/+}$ mice had a 14%
170 reduction in median lifespan compared to PS19 Tau mice and reached median survival 44 days
171 earlier then PS19 Tau mice. In addition, there was a further exacerbation of reduced lifespan as
172 pathology became more severe. PS19;*Lsd1*$^{\Delta/+}$ mice reached the point when there was only 10%
173 of the population remaining 83 days earlier than PS19 Tau mice, and all but one of the last 25%
174 of PS19;*Lsd1*$^{\Delta/+}$ mice died between 11.5-13.5 months, compared to 13.5-19 months in PS19 Tau
175 mice. As a result, 28% of PS19 Tau mice were still alive after all but one of the PS19;*Lsd1*$^{\Delta/+}$
176 mice had died (Fig. 2A).

177 PS19 Tau mice develop paralysis starting with hind limb clasping which progresses until
178 they are unable to feed (*28*). In our hands, PS19 Tau mice displayed intermittent hind limb
179 clasping starting at approximately 6 months of age. At 12 months, these mice had a severe clasp,
180 but were still mobile. This is delayed compared to what was originally reported by Yoshiyama
181 and colleagues (*28*). PS19;*Lsd1*$^{\Delta/+}$ mice also displayed intermittent hind limb clasping beginning
182 at approximately 6 months of age. However PS19;*Lsd1*$^{\Delta/+}$ mice became terminally paralyzed at a
183 faster rate compared to PS19 Tau mouse littermates. At 12 months, when PS19 Tau mice were
184 still mobile, PS19;*Lsd1*$^{\Delta/+}$ mice were severely paralyzed and typically terminal (Movie S1). To
185 quantitatively assess paralysis we performed rotarod and grid performance tests. In the rotarod,
186 we assessed the ability of the mice to stay on the rotating rod (latency to fall) (Fig. 2B), the speed
187 of the rod at which they fall off the rotarod (rotations per minute) (Fig. 2C), and the total distance
188 traveled (Fig. 2D). All genotypes performed the same at 6 months and 8 months (Fig. 2B-D).
189 However, at 10 months, when PS19 Tau mice still performed normally, PS19;*Lsd1*$^{\Delta/+}$ mice had a
190 significant deficit in mobility (P-value < 0.01, Fig. 2B,C). A deficit in PS19;*Lsd1*$^{\Delta/+}$ mice was

191 also observed at 10 months in the total distance traveled (Fig. 2D) and in grid performance
192 testing (Fig. S3 A), though neither were statistically significant.
193 To further investigate the exacerbation of paralysis we examined spinal cord motor
194 neurons. Healthy motor neurons from *Lsd1*$^{+/+}$ control mice express LSD1 (Fig. S3 B-D) and are
195 classically identified by circular nuclei at the center of a large cell body. In contrast to the
196 healthy motor neurons we observed in 12 month old PS19 Tau mice (Fig. S3 E), many of the
197 motor neurons in PS19;*Lsd1*$^{\Delta/+}$ mice at 12 months had abnormal morphology, with the nucleus
198 skewed to the edge of the cell body (Fig. S3 E vs. S3 F) and a ballooned cell body (Fig. S3 F).
199 Within the cell body we found aberrant hyperphosphorylated NFH (heavy chain neurofilament),
200 which is a sign of activated neuronal stress pathways (Fig S3 G vs. S3 H) (*36, 37*). This
201 abnormal morphology is highly reminiscent of a well-established process known as
202 chromatolysis, which is characterized by swelling of the neuronal cell body, disruption of Nissl
203 granules, and pyknotic or shrunken nuclei abnormally skewed to the edge of the cell body (*38,*
204 *39*). Chromatolysis, which is linked to neuronal stress and often leads to apoptosis (*39*), has been
205 observed in AD and other neurodegenerative diseases (*38, 40-42*).
206
207 **Reduction of LSD1 exacerbates PS19 Tau neurodegeneration**
208 In addition to accelerating the paralysis phenotype, reducing the level of *Lsd1* in PS19 Tau mice
209 exacerbated neuronal cell death in the brain. At 6 months and 8 months, we observed no
210 difference between genotypes in the overall morphology in the hippocampus (Fig. S4 A-H),
211 based on histological analysis. There was also no difference between *Lsd1*$^{+/+}$ and *Lsd1*$^{\Delta/+}$ mice at
212 10 months or 12 months (Fig. 3A,B; Fig. S4 I,J,M,N; Fig. S5 A,B,E,F,I,J,M,N). At 10 months,
213 PS19 Tau mice had very little cell loss in the hippocampus compared to *Lsd1*$^{+/+}$ and *Lsd1*$^{\Delta/+}$

214 control mice (Fig. S4 I-K, M-O). In contrast, at 10 months, PS19;*Lsd1*$^{\Delta/+}$ mice had dramatic cell
215 loss both in the CA1 region of the hippocampus and throughout the posterior hippocampus (Fig.
216 S4 L,P). At 12 months, the PS19 Tau mice had a slight decrease in CA1 and CA3 neurons
217 spanning the hippocampal pyramidal cell layer compared to *Lsd1*$^{+/+}$ control mice (17% and
218 19.4% respectively, Fig. 3A,B; Fig. S5 A-C, E-G). In comparison, PS19;*Lsd1*$^{\Delta/+}$ mice had a 52%
219 and 54% decrease in the CA1 and CA3 respectively (Fig. 3A,B; Fig. S5 D,H) compared to
220 *Lsd1*$^{+/+}$ control mice. This resulted in decreased overall brain size (Fig. 3C) and brain weight
221 (Fig. 3D) in PS19;*Lsd1*$^{\Delta/+}$ mice compared to PS19 Tau and *Lsd1*$^{\Delta/+}$ mouse littermates.
222 Additionally, at 12 months there were increased levels of cell loss in the Dentate Gyrus (Fig. S5
223 I-L), and throughout the posterior hippocampus (Fig. S5 M-P).
224 Along with the histology, we monitored the progression of neuronal cell death in the
225 same individual over time by performing magnetic resonance imaging (MRI) at 6 months and
226 again at 10 months (Movie S2). At 6 months, there was no sign of cell loss or ventricular
227 dilatation in *Lsd1*$^{\Delta/+}$, PS19 Tau, or PS19;*Lsd1*$^{\Delta/+}$ mice (Fig. 3E-G). However, at 10 months the
228 MRI showed that there was dramatic ventricular dilatation in PS19;*Lsd1*$^{\Delta/+}$ mice, as evidenced by
229 high-intensity areas in T2- weighted imaging, with substantial hippocampal and neocortical
230 atrophy (Fig. 3J vs. 3H, Movie S2). At this timepoint, PS19 Tau mice had some ventricular
231 dilatation and hippocampal atrophy throughout the hippocampus (Fig. 3I), but much less than
232 PS19;*Lsd1*$^{\Delta/+}$ mice (Fig. 3J, Movie S2. 0:51sec vs. 1:00sec).
233
234 **Tau pathology is not affected by change in LSD1 levels**
235 Since LSD1 is a chromatin regulator, it is possible that reducing LSD1 protein levels affects the
236 PS19 Tau transgene. However, we confirmed that there was no difference between PS19 Tau

237 mice and PS19;*Lsd1*$^{\Delta/+}$ mice in the endogenous mouse *Mapt* RNA expression, nor in the human
238 P301S MAPT transgene expression (Fig. S6 A). It is also possible that LSD1 affects tau
239 pathology. To test this, we performed immunohistochemistry staining for a hyperphosphorylated
240 form of tau (AT8). As expected, we did not observe any AT8 positive staining in *Lsd1*$^{\Delta/+}$ at 6, 8,
241 or 10 months (Fig. S6 B,E,H). Additionally, we observed very little AT8 positive
242 immunoreactivity at 6 months in both PS19 Tau or PS19;*Lsd1*$^{\Delta/+}$ mice (Fig. S6 C,D). At 8
243 months both PS19 Tau and PS19;*Lsd1*$^{\Delta/+}$ mice had low but consistent levels of AT8 positive
244 immunoreactivity (Fig. S6 F,G), and by 10 months both PS19 Tau and PS19;*Lsd1*$^{\Delta/+}$ mice
245 developed the same high level of AT8 positive tau immunoreactivity (Fig. S6 I,J). This was
246 consistent throughout both the CA1 and CA3 regions of the hippocampus and the cerebral cortex
247 (Fig. S6 K-M). We also did not observe any difference between PS19 Tau mice and
248 PS19;*Lsd1*$^{\Delta/+}$ mice when assaying PHF1 (an alternative phospho-tau antibody) immunoreactivity
249 in the CA1 region of the hippocampus at 8 months (Fig. S7 A-C, G) and 10 months (Fig. S7 D-F,
250 G), nor in the CA3 region of the hippocampus or the cerebral cortex at 8 and 10 months (Fig. S7
251 H,I).
252
253 **The functional interaction between tau pathology and LSD1 inhibition is specific**
254 To test the specificity of the functional interaction between tau pathology and LSD1, we
255 investigated the overlap in the effected molecular pathways associated with both pathological tau
256 and *Lsd1* heterozygosity. To address this, we performed RNA sequencing on the hippocampus of
257 9 month *Lsd1*$^{+/+}$, *Lsd1*$^{\Delta/+}$, PS19 Tau, and PS19;*Lsd1*$^{\Delta/+}$ littermates. As opposed to analyzing
258 transcriptional changes at the terminal stage of disease, this time point allows us to assess
259 molecular changes prior to the onset of neuronal cell death. This is also the time point that we

260 observed the earliest signs of exacerbation of paralysis in PS19;*Lsd1*$^{\Delta/+}$ mice. Because of this
261 early stage in the progression of the disease, we would not expect dramatic changes in
262 transcription overall. Nevertheless, if tau pathology is inhibiting LSD1 function, we would
263 expect that the genome-wide expression changes induced by tau might be exacerbated by a
264 reduction in LSD1. The RNA-seq analysis detected 112 significant gene expression changes in
265 PS19 Tau mice compared to *Lsd1*$^{+/+}$ (Fig S8 A,B), and 295 significant gene expression changes
266 in PS19;*Lsd1*$^{\Delta/+}$ mice compared to *Lsd1*$^{+/+}$ (Fig S8 C,D). Importantly, *Lsd1*$^{\Delta/+}$ mice had only 4
267 gene expression changes observed genome-wide (Fig. S8 E,F), indicating that the partially
268 reduced level of LSD1 expression had very little effect on transcription on its own. This is
269 consistent with the lack of phenotype in these animals.

270 We first examined the relationship between tau-induced expression changes and the
271 effects of *Lsd1* heterozygosity by comparing the transcriptional changes observed in PS19 Tau
272 mice with PS19;*Lsd1*$^{\Delta/+}$ mice. In PS19 Tau mice that do not yet have significant
273 neurodegeneration, we identified 112 genes (107 up and 5 down) that were differentially
274 expressed. All of these 112 genes were changed in the same direction in PS19;*Lsd1*$^{\Delta/+}$ mice. In
275 addition, amongst the 112 genes changed in the same direction, 104 (93%) had exacerbated
276 expression in PS19;*Lsd1*$^{\Delta/+}$ mice compared to PS19 Tau mice (Fig. 4A). Based on this overlap,
277 we further compared the expression changes between PS19 Tau mice and PS19;*Lsd1*$^{\Delta/+}$ mice
278 genome-wide. Amongst the transcripts that were changed in both PS19 Tau mice and
279 PS19;*Lsd1*$^{\Delta/+}$ mice compared to *Lsd1*$^{+/+}$ mice, 77% changed in the same direction (either up or
280 down). Consistent with this overlap in gene expression, Gene Set Enrichment Analysis
281 demonstrated that the pathways that are affected in both PS19 Tau mice and PS19;*Lsd1*$^{\Delta/+}$ mice
282 are very similar (Fig. S8 G-J). However, the genes affected in both sets of mice tended to be

283 further exacerbated in PS19;*Lsd1*$^{\Delta/+}$ mice compared to PS19 Tau mice. Amongst the 77% of
284 genes that changed in the same direction in both PS19 Tau mice and PS19;*Lsd1*$^{\Delta/+}$ mice, 75% of
285 these transcripts had a higher fold-change in PS19;*Lsd1*$^{\Delta/+}$ mice compared to PS19 Tau mice
286 (Fig. 4B). Importantly, the gene expression pathways that are induced by the PS19 transgene
287 overlap substantially with those observed in human AD case **(***43***)**. This suggests that reduction of
288 *Lsd1* exacerbates human AD pathways.
289
290 **Overexpression of LSD1 rescues neurodegeneration in the hippocampus of PS19 Tau mice**
291 Our data demonstrate that reduction of LSD1 protein exacerbates the tauopathy phenotype in
292 PS19 Tau mice. Based on this, we considered the possibility that overexpression of LSD1 might
293 counter the loss of LSD1 from the nucleus and protect against neurodegeneration in PS19 Tau
294 mice. To address this possibility, we injected PS19 Tau mice with a neuronal specific virus
295 (AAV-DJ driven by the synapsin promoter) expressing either the full length LSD1 protein with
296 an N-terminal HA tag (hereafter referred to as PS19- LSD1 inj) or a control virus expressing
297 only the HA tag (hereafter referred to as PS19- HA inj). Additionally, to control for the effects of
298 viral injection, we injected Wild Type littermates with the HA only expressing virus (hereafter
299 referred to as WT- HA inj). All injections were performed directly into the hippocampus at 8-8.5
300 months, when tau pathology is already present throughout the nervous system. Immunolabeling
301 for the HA tag demonstrated that the virus is specific to NeuN+ neurons (Fig. S9 A-D), with no
302 HA expression observed in IBA+ microglia (Fig. S9 E-H), or GFAP+ astrocytes (Fig. S9 I-L). It
303 also confirmed that virally expressed LSD1 is nuclear (Fig. S9 M) and confined to the
304 hippocampus (Fig. S9 N), even at 11-11.5 months, when LSD1 is normally becoming
305 sequestered to the cytoplasm (Fig. S9 O-R). After 3 months of overexpression, 11-11.5 month

306 old mice were euthanized, and the brains were analyzed. Injections resulted in a ~6-fold increase
307 in expression of LSD1 in the hippocampus compared to endogenous LSD1 in the PS19- HA inj
308 mice, but no increase in the cerebellum (Fig. S9 S,T). As expected, because the viral injections
309 were restricted to the hippocampus, the mice injected with LSD1 still developed paralysis
310 (Movie S3). This confirms that the tau transgene is expressed and functioning. Additionally, we
311 did not observe a difference in total levels of AT8 positive tau immunoreactivity (Fig. S9 U-X).
312 Therefore, any modulation to the phenotype was not due to changes in tau pathology.
313 Injected mice were evaluated for cell death by neuronal cell counts in the hippocampus.
314 Injection of LSD1 virus into the hippocampus of PS19 Tau mice rescued the neurodegeneration
315 phenotype. At 11 months, compared to WT-HA inj control mice, 70% of the PS19-HA inj mice
316 had hippocampal cell counts that were below the lowest WT-HA inj control, while none of the
317 Tau mice injected with the LSD1 virus were below this level. Overall, we observed significantly
318 more neurons (P-value <0.05) spanning the pyramidal cell layer (84% of WT- HA inj CA1
319 counts) compared to their PS19- HA inj littermates (59% of WT- HA inj CA1 counts), such that
320 overall the neuronal cell count in PS19- LSD1 inj mice was not statistically different from the
321 WT- HA inj (Fig. 5A-D). Additionally, in the histological analysis we observed a large number
322 of cells infiltrating the hippocampus in PS19- HA inj mice compared to WT- HA inj littermates
323 (Fig. 5B vs. 5C). Marker analysis demonstrated that this was due to a strong inflammatory
324 response, with a large increase in the number of GFAP+ astrocytes (Fig. S10 A-C vs. D-F) and
325 TRL2+ activated microglia (Fig. S10 J-L vs. M-O, S-V vs. W,Z, EE). Injection of PS19 Tau
326 mice with LSD1 virus rescued this inflammatory response. For example, all but one (9 out of 10
327 analyzed) of the PS19- LSD1 inj mice had a reduction in the number of GFAP+ astrocytes (Fig.
328 S10 G-I vs. D-F) and TRL2+ activated microglia (Fig. S10 P-R vs. M-O, AA-DD vs. W-Z, EE).

329 Of note, the one PS19- LSD1 inj mouse where we did observe increased glial cells, similar to
330 PS19- HA inj mice, had the lowest neuronal cell count (74% of WT- HA inj CA1 neurons). It is
331 possible that this mouse was already undergoing neurodegeneration prior to the injection of the
332 LSD1 overexpression virus.

333 Although the number of hippocampal neurons in PS19- LSD1 inj mice did not differ
334 from WT- HA inj controls, in 6 of the 10 PS19- LSD1 inj mice we observed cells with abnormal
335 blebbed nuclei at varying numbers throughout the hippocampus (Fig. 5E). These abnormal cells
336 are rare in PS19- HA inj mice, which have a reduced overall number of cells in the pyramidal
337 cell layer compared to WT- HA inj control mice. One possibility is that these abnormal cells
338 with blebbing nuclei represent an intermediate state between a healthy neuron and a dying
339 neuron that is prolonged by rescue via LSD1 overexpression. Interestingly, these abnormal cells
340 also differed in the localization of HA-tagged LSD1. The four mice with normal nuclei had HA-
341 tagged LSD1 protein localized uniformly throughout the nucleus (Fig. 5F). In contrast, the six
342 mice with abnormal nuclear blebbing had some HA-tagged LSD1 that was mislocalized to the
343 cytoplasm (Fig. 5G). This includes the one PS19- LSD1 inj mouse that had an elevated number
344 of astrocytes and TRL2 positive microglia. Thus, the blebbing state correlates with when the
345 viral produced LSD1 begins to be sequestered in the cytoplasm, similar to the endogenously
346 produced LSD1.

347 To test the specificity of the rescue that we observe when LSD1 is overexpressed in the
348 hippocampus of PS19 Tau mice, we performed RNA sequencing on the hippocampus of rescued
349 11-11.5 month old PS19- LSD1 inj mice versus PS19- HA inj mice. The RNA-seq analysis
350 detected 144 significant gene expression changes PS19- HA inj mice compared to WT- HA inj
351 control mice (Fig. S11 A,B), and 57 significant gene expression changes in PS19- LSD1 inj mice

352 compared to WT- HA inj control mice (Fig. S11 C,D). All of the 144 significant gene expression
353 changes induced by tau are ameliorated by overexpression of LSD1 (Fig. 6A). As a result, 116
354 out of the 144 significantly changed genes in the PS19 Tau- HA mice are no longer significantly
355 changed in the rescued PS19- LSD1 inj mice. Based on this specific rescue of the differentially
356 expressed genes induced by tau, we further compared the expression changes between PS19-
357 LSD1 inj mice and PS19- HA inj mice genome-wide (Fig. 6B). Amongst the genome-wide
358 expression changes in PS19- HA inj mice compared to WT- HA inj control mice, 76% were
359 changed in the same direction (either up or down), and of these 69% were ameliorated. It should
360 be noted, that this is the opposite of what we observe when we reduce LSD1 (Fig. 4). Thus, tau-
361 induced gene expression changes can be specifically modulated in both directions by increasing
362 or decreasing LSD1 levels. Importantly, the pathways identified by Gene Set Enrichment
363 Analysis are similar between PS19- LSD1 inj mice and PS19- HA inj mice, and we fail to detect
364 any new pathways induced by overexpression of LSD1 that could potentially account for a non-
365 specific rescue (Fig. S11 E-H).
366

367 **DISCUSSION**

368 In this study we investigate a potential downstream mediator of tau pathology in
369 neurodegenerative disease. We find that modulation of the chromatin modifying enzyme LSD1
370 can alter neurodegeneration in a tauopathy mouse model. Previously, we showed that LSD1
371 colocalizes with tau pathology in the cell body of neurons in AD cases (*26*). This suggested that
372 LSD1 might be disrupted in tauopathies such as AD, by being excluded from the nucleus. To
373 address this directly, we utilize the PS19 tauopathy mouse model. In these mice, we find that
374 LSD1 is sequestered in the cytoplasm, in some cases being completely depleted from the

375 nucleus. This provides the first cytological evidence that pathological tau can prevent LSD1 from
376 properly localizing to the nucleus in hippocampal and cortical neurons, where we have
377 previously shown it is continuously required (*44*).

378 Based on the ability of pathological tau to sequester LSD1, we hypothesized that
379 neuronal cell death may be due, at least partly, to LSD1 being sequestered in the cytoplasm and
380 depleted from the nucleus. In this case, reducing LSD1 levels should make it easier for tau to
381 deplete LSD1 from the nucleus, resulting in a faster progression of neurodegeneration and/or a
382 more severe neurodegenerative phenotype. We find that reducing LSD1 in the PS19 Tau
383 transgenic background accelerates the depletion of LSD1 from the nucleus compared to PS19
384 Tau mice alone. Surprisingly, in PS19;*Lsd1*$^{\Delta/+}$ mice we also observe a slight decrease in number
385 of cells in the cortex with LSD1 localized completely to the cytoplasm. However, this is likely
386 because many of the cells in mice with decreased LSD1 have died and been cleared. Consistent
387 with this possibility, we observe less cells/area overall in PS19;*Lsd1*$^{\Delta/+}$ mice compared to PS19
388 Tau mice.

389 LSD1 heterozygosity alone induces only 4 significant gene expression changes and does
390 not lead to any neurodegeneration. This suggests that any effects observed in PS19;*Lsd1*$^{\Delta/+}$ mice
391 are not simply due to LSD1 haploinsufficiency. Normally, PS19 Tau mice develop paralysis and
392 neurodegeneration, along with reduced survival. When we reduce LSD1 in the PS19 Tau mice,
393 mice die significantly earlier, most likely due to the increased rate of paralysis. Additionally,
394 PS19;*Lsd1*$^{\Delta/+}$ mice have increased neuronal cell death and clearance in the hippocampus. This
395 suggests that pathological tau functions through LSD1 to cause neurodegeneration *in vivo* in
396 mice.

397 PS19;*Lsd1*$^{\Delta/+}$ mice have a 31% reduction in LSD1 protein levels compared to PS19 Tau
398 mice from birth. This reduction should theoretically make mice sensitive to LSD1 depletion from
399 birth. However, tau pathology starts at 6-8 months in PS19 Tau mice. As a result, if *Lsd1*
400 heterozygosity is functioning by making it easier for pathological tau to deplete LSD1 from the
401 nucleus, we would not expect to see any exacerbation until after pathological tau is present. The
402 exacerbation of the PS19 Tau mouse neurodegenerative phenotype does not occur until after
403 pathological human tau was present. This suggests that the effect of *Lsd1* heterozygosity requires
404 the presence of pathological tau, placing LSD1 downstream of tau. Consistent with LSD1 being
405 downstream of pathological tau, we found no evidence that *Lsd1* heterozygosity affects the
406 expression of the tau transgene, or the buildup of pathological tau in PS19 Tau mice.
407 To test whether the functional interaction between pathological tau and reduced LSD1 is
408 specific, we used RNA-seq to determine whether the downstream molecular pathways altered in
409 PS19 Tau mice are exacerbated in PS19;*Lsd1*$^{\Delta/+}$ mice. This analysis was performed at the time of
410 earliest signs of neuronal distress, allowing us to assess molecular changes prior to cell death and
411 clearance. LSD1 heterozygosity induces only 4 significant expression changes. In addition, the
412 pathways that are affected in both PS19 Tau mice and PS19;*Lsd1*$^{\Delta/+}$ mice are very similar. This
413 suggests that reducing LSD1 did not induce any additional neurodegeneration pathways. In
414 contrast, when LSD1 is reduced in PS19 Tau mice, the genome-wide expression changes
415 induced by pathological tau are specifically exacerbated. This suggests that the functional
416 interaction that we observe between pathological tau and reduced LSD1 is occurring through the
417 tau pathway.
418 Our previous data implicated LSD1 in the tau-mediated neurodegeneration pathway.
419 Utilizing the PS19 Tau mouse model, we now show a functional interaction between

420 pathological tau and LSD1. Importantly, because the tau mutation utilized in PS19 Tau mice
421 comes from an FTD patient, the functional interaction that we detected may also be relevant to
422 FTD and other taupathies, such progressive supranuclear palsy, corticobasal degeneration and
423 chronic traumatic encephalopathy. However, because PS19 Tau mice do not have Aβ plaque
424 accumulation, this functional interaction would not be relevant to dysfunction induced directly
425 by pathological Aβ.

426 Based on the data we uncovered showing a specific functional interaction between
427 pathological tau and LSD1, we propose the following model (Movie S4): in healthy hippocampal
428 and cortical neurons, LSD1 is translated in the cytoplasm and transported into the nucleus where
429 it is continuously required to repress inappropriate transcription. In tauopathy, pathological tau
430 accumulates in the cytoplasm blocking LSD1 from nuclear import. This interferes with the
431 continuous requirement for LSD1, resulting in neuronal cell death. It is possible that pathological
432 tau inhibits LSD1 function indirectly, by interfering with some other process that subsequently
433 disrupts LSD1 function. However, based on our observations that LSD1 mislocalizes to
434 cytoplasmic pathological tau in PS19 Tau mice and human AD cases (*44*), we favor a model
435 where pathological tau directly masks LSD1 from interacting with the nuclear import complex.
436 Regardless of whether the interaction is direct or indirect, it should be noted that breakdown of
437 the nuclear pore, which has been observed in human AD cases (*45-47*), would potentially
438 exacerbate the model that we propose.

439 This model makes a direct prediction: if tau is predominantly functioning through LSD1,
440 then increasing the levels of LSD1 should rescue the tau-induced neurodegenerative phenotype.
441 To address this, we overexpressed LSD1 in the hippocampal neurons of PS19 Tau mice.
442 Overexpression of LSD1 specifically in hippocampal neurons rescues the neuronal cell death and

443 limits the inflammatory response. This rescue is neuronal specific, suggesting that the functional
444 interaction between LSD1 and tau is occurring in neurons. In addition, this rescue occurs despite
445 there being no effect on tau aggregation. This negates the possibility that the tau transgene is
446 simply not functioning when LSD1 is overexpressed. The ability of LSD1 overexpression to
447 overcome tau-mediated neurodegeneration in the presence of pathological tau aggregates,
448 provides further evidence that pathological tau is functioning through the inhibition of LSD1.

449 *A priori*, we would not expect the gene expression changes induced by overexpression of
450 LSD1 to be related to the gene expression changes induced by pathological tau. However, the
451 data presented here, along with our previous work (*44*), raise the possibility that pathological tau
452 may be causing neurodegeneration by sequestering and inhibiting tau. If this is the case, we
453 would expect that overexpression of LSD1, even after pathological tau is present, would
454 specifically counteract tau-induced expression changes. Strikingly, we find that overexpression
455 of LSD1 ameliorates tau-induced gene expression changes genome-wide. This suggests that the
456 inhibition of LSD1 may be the critical mediator of neurodegeneration caused by pathological tau.

457 Overexpressing LSD1 should not prevent it from being sequestered. Rather
458 overexpressing LSD1 should make it more difficult for pathological tau to sequester all of the
459 LSD1 protein, allowing some LSD1 to be transported to the nucleus. Thus, overexpressing LSD1
460 would be expected to temporarily rescue the ability of pathological tau to kill neurons.
461 Consistent with this, LSD1 overexpression delays the effect of pathological tau rather than
462 permanently rescuing. In 60% of the mice, the surviving neurons have abnormal morphology,
463 and the overexpressed version of LSD1 is also sequestered. The observation that neurons fail to
464 maintain their morphology when the overexpressed LSD1 begins to be sequestered in the
465 cytoplasm provides further support for the model that tau mediates neurodegeneration through

466 the sequestration of LSD1. Nevertheless, our data suggest that overexpression of LSD1 cannot
467 permanently overcome pathological tau. To permanently overcome pathological tau, it would
468 likely be necessary to permanently disrupt the interaction between pathological tau and LSD1.
469 This work is currently ongoing in the lab. Overall, our data establish LSD1 as a major
470 downstream effector of tau-induced neurodegeneration. Based on these data, we propose that the
471 LSD1 pathway is a potential late stage target for intervention in tauopathies, such as AD.

472

473 **MATERIALS AND METHODS**

474 The mouse strains are described in SI Materials and Methods. All relevant techniques are also
475 included there. These include mouse tissue fixation, histology and histological studies,
476 immunohistochemistry and immunofluorescence, protein quantification, quantitative analysis of
477 paralysis, MRI of brain atrophy, RNA sequencing, RNA sequencing analysis, stereotaxic surgery
478 and viral infusion, and statistical analysis.

479

480 **ACKNOWLEDGMENTS**

481 We thank M. Rosenfeld (U.C.S.D) for providing *Lsd1* deletion mice and D. Castrillon for
482 providing the *Vasa-Cre* mice; N. Seyfried, R. Betarbet, Mr. Gearing, from the Emory ADRC
483 (P50 AG025688), NINDS Emory Neuroscience Core Facilities (P30NS055077) for tissue
484 processing and providing PHF1 antibody, J. Alcudia of the Stanford Gene Vector and Virus Core
485 for the help with virus generation and production, the Georgia Genomics and Bioinformatics
486 Core, which provided the RNA library preparation and sequencing service, J. Schroeder from
487 Emory Rodent Behavioral Core for help with Rotatord and Grid Performance assays supported
488 by the Emory Neuroscience NINDS Core Facilities (P30NS055077) with further support

489 provided by the Georgia Clinical & Translational Science Alliance of the National Institutes of
490 Health under Award Number UL1TR002378; and J. Park from the Emory Center for Systems
491 Imagining for preforming MRI supported by the National Center for Advancing Translational
492 Sciences of the National Institutes of Health under Award Number UL1TR000454**.** We would
493 also like to thank M.J. Rowley and V. Corces for assistance on RNA sequencing analysis, K.
494 Porter-Stransky and D. Weinshenker for providing PS19 Tau mouse and teaching stereotaxic
495 surgery procedure, L.R. Lym and Dr. Lerit for assistance with confocal imagining; D.
496 Weinshenker, A. Levey, C. Bean and T. Caspary for comments on the manuscript and assistance
497 throughout. Additionally the authors would like to thank fellow Katz lab members for assistance
498 experimentally and intellectually. **Funding:** A.K.E was supported by the National Institute of
499 General Medicine training grant (T32 GM008367-26) and an NRSA from National Institute of
500 Neurological Disorders and Stroke (NINDS) (F31 NS098663-02). D.A.M was supported by a
501 research supplement to promote diversity in health-related research from the NINDS
502 (1R01NS087142). S.M.K was supported the NINDS Training in Translational Research in
503 Neurology grant (5T32 NS007480-17). M.J.R. is supported by the National Institutes of Health
504 (NIH) Pathway to Independence Award K99/R00 GM127671.The work was supported by a
505 grant to D.J.K from the National Institute of Neurological Disorders and Stroke
506 (1R01NS087142). **Competing Interests:** The authors declare that they have no competing
507 interests. **Data and materials availability:** FastQ files for the RNA sequencing experiments are
508 bring deposited in the GEO and will be available upon publication. Results from DESEQ2 are
509 available in Data S1. Correspondence and requests for materials should be addressed to D.J.K.
510 (djkatz@emory.edu).
511

REFERENCES

1. M. E. Orr, A. C. Sullivan, B. Frost, A Brief Overview of Tauopathy: Causes, Consequences, and Therapeutic Strategies. *Trends in pharmacological sciences* **38**, 637-648 (2017).
2. Y. Wang, E. Mandelkow, Tau in physiology and pathology. *Nat Rev Neurosci* **17**, 5-21 (2016).
3. D. M. Holtzman *et al.*, Tau: From research to clinical development. *Alzheimers Dement* **12**, 1033-1039 (2016).
4. C. M. Wischik *et al.*, Isolation of a fragment of tau derived from the core of the paired helical filament of Alzheimer disease. *Proc Natl Acad Sci U S A* **85**, 4506-4510 (1988).
5. M. Goedert, C. M. Wischik, R. A. Crowther, J. E. Walker, A. Klug, Cloning and sequencing of the cDNA encoding a core protein of the paired helical filament of Alzheimer disease: identification as the microtubule-associated protein tau. *Proc Natl Acad Sci U S A* **85**, 4051-4055 (1988).
6. J. Hardy, D. J. Selkoe, The amyloid hypothesis of Alzheimer's disease: progress and problems on the road to therapeutics. *Science* **297**, 353-356 (2002).
7. S. H. Barage, K. D. Sonawane, Amyloid cascade hypothesis: Pathogenesis and therapeutic strategies in Alzheimer's disease. *Neuropeptides* **52**, 1-18.
8. G. S. Bloom, Amyloid-β and Tau: The Trigger and Bullet in Alzheimer Disease PathogenesisAmyloid-β and TauAmyloid-β and Tau. *JAMA Neurology* **71**, 505-508 (2014).
9. C. Duyckaerts, B. Delatour, M.-C. Potier, Classification and basic pathology of Alzheimer disease. *Acta Neuropathologica* **118**, 5-36 (2009).
10. P. V. Arriagada, J. H. Growdon, E. T. Hedley-Whyte, B. T. Hyman, Neurofibrillary tangles but not senile plaques parallel duration and severity of Alzheimer's disease. *Neurology* **42**, 631-639 (1992).
11. E. Karran, M. Mercken, B. De Strooper, The amyloid cascade hypothesis for Alzheimer's disease: an appraisal for the development of therapeutics. *Nat Rev Drug Discov* **10**, 698-712 (2011).
12. T. Gomez-Isla *et al.*, Neuronal loss correlates with but exceeds neurofibrillary tangles in Alzheimer's disease. *Ann Neurol* **41**, 17-24 (1997).
13. A. Bejanin *et al.*, Tau pathology and neurodegeneration contribute to cognitive impairment in Alzheimer's disease. *Brain* **140**, 3286-3300 (2017).
14. D. E. Hurtado *et al.*, A{beta} accelerates the spatiotemporal progression of tau pathology and augments tau amyloidosis in an Alzheimer mouse model. *Am J Pathol* **177**, 1977-1988 (2010).
15. Z. He *et al.*, Amyloid-beta plaques enhance Alzheimer's brain tau-seeded pathologies by facilitating neuritic plaque tau aggregation. *Nat Med* **24**, 29-38 (2018).
16. S. H. Choi *et al.*, A three-dimensional human neural cell culture model of Alzheimer/'s disease. *Nature* **515**, 274-278 (2014).
17. H. Braak, E. Braak, Frequency of Stages of Alzheimer-Related Lesions in Different Age Categories. *Neurobiology of Aging* **18**, 351-357 (1997).
18. D. P. Hanger, J. C. Betts, T. L. Loviny, W. P. Blackstock, B. H. Anderton, New phosphorylation sites identified in hyperphosphorylated tau (paired helical filament-tau) from Alzheimer's disease brain using nanoelectrospray mass spectrometry. *J Neurochem* **71**, 2465-2476 (1998).
19. M. Morishima-Kawashima *et al.*, Hyperphosphorylation of tau in PHF. *Neurobiol Aging* **16**, 365-371; discussion 371-380 (1995).
20. T. Arendt, J. T. Stieler, M. Holzer, Tau and tauopathies. *Brain Research Bulletin* **126**, 238-292 (2016).

562 21. R. J. Castellani, G. Perry, Tau Biology, Tauopathy, Traumatic Brain Injury, and
563 Diagnostic Challenges. *J Alzheimers Dis* **67**, 447-467 (2019).
564 22. E. Masliah *et al.*, Altered expression of synaptic proteins occurs early during progression
565 of Alzheimer's disease. *Neurology* **56**, 127-129 (2001).
566 23. M. Ingelsson *et al.*, Early Abeta accumulation and progressive synaptic loss, gliosis, and
567 tangle formation in AD brain. *Neurology* **62**, 925-931 (2004).
568 24. J. W. Kinney *et al.*, Inflammation as a central mechanism in Alzheimer's disease.
569 *Alzheimer's & Dementia: Translational Research & Clinical Interventions* **4**, 575-590
570 (2018).
571 25. J. M. Rubio-Perez, J. M. Morillas-Ruiz, A review: inflammatory process in Alzheimer's
572 disease, role of cytokines. *TheScientificWorldJournal* **2012**, 756357-756357 (2012).
573 26. M. A. Christopher *et al.*, LSD1 protects against hippocampal and cortical
574 neurodegeneration. *Nature Communications* **8**, 805 (2017).
575 27. Y. Jin *et al.*, Nuclear import of human histone lysine-specific demethylase LSD1. *J*
576 *Biochem* **156**, 305-313 (2014).
577 28. Y. Yoshiyama *et al.*, Synapse Loss and Microglial Activation Precede Tangles in a
578 P301S Tauopathy Mouse Model. *Neuron* **53**, 337-351.
579 29. A. Bellucci *et al.*, Induction of Inflammatory Mediators and Microglial Activation in Mice
580 Transgenic for Mutant Human P301S Tau Protein. *The American Journal of Pathology*
581 **165**, 1643-1652 (2004).
582 30. M. Iba *et al.*, Tau pathology spread in PS19 tau transgenic mice following locus
583 coeruleus (LC) injections of synthetic tau fibrils is determined by the LC's afferent and
584 efferent connections. *Acta Neuropathol* **130**, 349-362 (2015).
585 31. T. Gallardo, L. Shirley, G. B. John, D. H. Castrillon, Generation of a germ cell-specific
586 mouse transgenic Cre line, Vasa-Cre. *Genesis (New York, N.Y. : 2000)* **45**, 413-417
587 (2007).
588 32. J. Wang *et al.*, Opposing LSD1 complexes function in developmental gene activation
589 and repression programmes. *Nature* **446**, 882-887 (2007).
590 33. D. B. Lyons *et al.*, An epigenetic trap stabilizes singular olfactory receptor expression.
591 *Cell* **154**, 325-336 (2013).
592 34. C. T. Foster *et al.*, Lysine-specific demethylase 1 regulates the embryonic transcriptome
593 and CoREST stability. *Molecular and cellular biology* **30**, 4851-4863 (2010).
594 35. L. Jin *et al.*, Loss of LSD1 (lysine-specific demethylase 1) suppresses growth and alters
595 gene expression of human colon cancer cells in a p53- and DNMT1(DNA
596 methyltransferase 1)-independent manner. *The Biochemical journal* **449**, 459-468
597 (2013).
598 36. B. I. Giasson, W. E. Mushynski, Aberrant stress-induced phosphorylation of perikaryal
599 neurofilaments. *J Biol Chem* **271**, 30404-30409 (1996).
600 37. Y. L. Liu *et al.*, Alternation of neurofilaments in immune-mediated injury of spinal cord
601 motor neurons. *Spinal Cord* **47**, 166 (2008).
602 38. L. D. F. Moon, Chromatolysis: Do injured axons regenerate poorly when ribonucleases
603 attack rough endoplasmic reticulum, ribosomes and RNA? *Dev Neurobiol* **78**, 1011-1024
604 (2018).
605 39. B. G. Cragg, What is the signal for chromatolysis? *Brain Res* **23**, 1-21 (1970).
606 40. S. Sil, A. R. Goswami, G. Dutta, T. Ghosh, Effects of naproxen on immune responses in
607 a colchicine-induced rat model of Alzheimer's disease. *Neuroimmunomodulation* **21**,
608 304-321 (2014).
609 41. J. Riancho *et al.*, Compensatory Motor Neuron Response to Chromatolysis in the Murine
610 hSOD1(G93A) Model of Amyotrophic Lateral Sclerosis. *Front Cell Neurosci* **8**, 346
611 (2014).

42. A. M. Cataldo, D. J. Hamilton, R. A. Nixon, Lysosomal abnormalities in degenerating neurons link neuronal compromise to senile plaque development in Alzheimer disease. *Brain Res* **640**, 68-80 (1994).
43. Y.-W. Wan *et al.*, Meta-Analysis of the Alzheimer's Disease Human Brain Transcriptome and Functional Dissection in Mouse Models. *Cell Reports* **32**, 107908 (2020).
44. M. A. Christopher *et al.*, LSD1 protects against hippocampal and cortical neurodegeneration. *Nat Commun* **8**, 805 (2017).
45. B. Eftekharzadeh *et al.*, Tau Protein Disrupts Nucleocytoplasmic Transport in Alzheimer's Disease. *Neuron* **99**, 925-940.e927 (2018).
46. L. G. Sheffield, H. B. Miskiewicz, L. B. Tannenbaum, S. S. Mirra, Nuclear Pore Complex Proteins in Alzheimer Disease. *Journal of Neuropathology & Experimental Neurology* **65**, 45-54 (2006).
47. B. Frost, F. H. Bardai, M. B. Feany, Lamin Dysfunction Mediates Neurodegeneration in Tauopathies. *Curr Biol* **26**, 129-136 (2016).
48. E. Afgan *et al.*, The Galaxy platform for accessible, reproducible and collaborative biomedical analyses: 2016 update. *Nucleic Acids Res* **44**, W3-w10 (2016).
49. E. Afgan *et al.*, The Galaxy platform for accessible, reproducible and collaborative biomedical analyses: 2018 update. *Nucleic Acids Research* **46**, W537-W544 (2018).
50. B. B. Gregory R. Warens, Lodewijk Bonebakker, Robert Gentleman, Wolfgang Huber Andy Liaw, Thomas Lumley, Martin Maechler, Arni Magnusson, Steffen Moeller, Marc Schwartz, Bill Venables. (2019).
51. K. Blighe, in *R. package version 1.2.0*. (2019).
52. J. Wang, D. Duncan, Z. Shi, B. Zhang, WEB-based GEne SeT AnaLysis Toolkit (WebGestalt): update 2013. *Nucleic Acids Res* **41**, W77-83 (2013).
53. J. Wang, S. Vasaikar, Z. Shi, M. Greer, B. Zhang, WebGestalt 2017: a more comprehensive, powerful, flexible and interactive gene set enrichment analysis toolkit. *Nucleic Acids Res* **45**, W130-w137 (2017).
54. Y. Liao, J. Wang, E. J. Jaehnig, Z. Shi, B. Zhang, WebGestalt 2019: gene set analysis toolkit with revamped UIs and APIs. *Nucleic Acids Res* **47**, W199-w205 (2019).
55. B. Zhang, S. Kirov, J. Snoddy, WebGestalt: an integrated system for exploring gene sets in various biological contexts. *Nucleic Acids Res* **33**, W741-748 (2005).

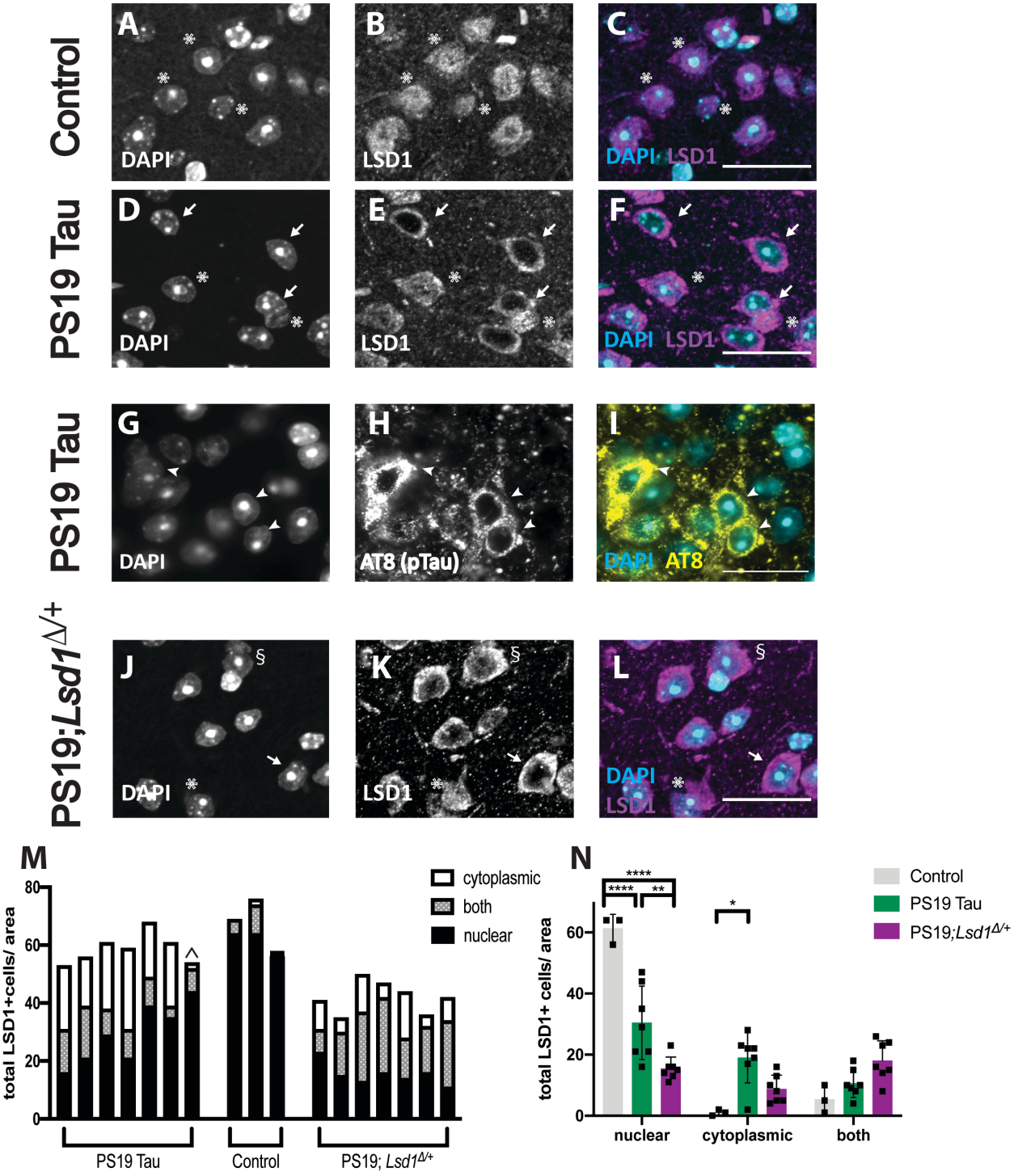
Control
PS19 Tau
PS19 Tau
PS19;Lsd1Δ/+
A
B
C
DAPI
LSD1
DAPI LSD1
D
E
F
DAPI
LSD1
DAPI LSD1
G
H
I
DAPI
AT8 (pTau)
DAPI AT8
J
K
L
§
DAPI
LSD1
DAPI
LSD1
M
cytoplasmic
both
nuclear
total LSD1+cells/ area
PS19 Tau
Control
PS19; Lsd1Δ/+
N
Control
PS19 Tau
PS19;Lsd1Δ/+
total LSD1+ cells/ area
nuclear
cytoplasmic
both

644

645 **Fig. 1: LSD1 sequestration and tau accumulation in the presence of pathological tau. A-C**, Representative
646 immunofluorescence of 12 month old control Wild Type mice showing DAPI (**A**), LSD1 (**B**), and merged (**C**) in the
647 cerebral cortex where LSD1 is localized specifically to DAPI positive nuclei. **D-F**, Representative image of the
648 cerebral cortex in 12 month old PS19 Tau mice. Staining for DAPI (**D**), LSD1 (**E**), and merged (**F**) shows that LSD1
649 is localized outside the nucleus, and depleted from the DAPI positive nucleus. Arrows denote cells where LSD1 is
650 localized outside of the nucleus, and asterisks denote LSD1 localized specifically to the nucleus. **G-I,** Representative
651 immunofluorescence of 12 month old PS19 Tau mouse with staining for DAPI (**G**), AT8 positive hyper-
652 phosphorylated tau (**H**) and merge (**I**) where hyper-phosphorylated tau accumulates in the cytoplasm of the cell
653 body. Arrowheads denote hyper-phosphorylated tau. **J-L,** Representative immunofluorescence of 12 month old
654 control Tau mice that are heterozygous for *Lsd1* (PS19; $Lsd1^{\Delta/+}$) showing DAPI (**J**), LSD1 (**K**), and merged (**L**) in
655 the cerebral cortex. Arrows denote cells where LSD1 is localized outside of the nucleus, asterisks denote LSD1
656 localized specifically inside the nucleus, and § denotes cells where LSD1 is both nuclear and cytoplasmic. Scale
657 bars=25µm. **M,N**, Quantification of the LSD1 localization represented in **A-F, J-L**.(**M**) Each bar represents a single
658 mouse. LSD1 was scored as being localized to the nucleus, the cytoplasm, or both areas. ^ denotes the one PS19 Tau
659 mouse with low levels of observed cytoplasmic LSD1 localization. (**N**) Combined analysis from **M** in each cell
660 region for Control (WT n=3), PS19 Tau (n=7), and PS19;$Lsd1^{\Delta/+}$ (n=7) mice. Values are mean ± SEM, two-way
661 analysis of variance (ANOVA) with Tukey's post hoc test *P<0.05, **P<0.01,****P<0.001.
662

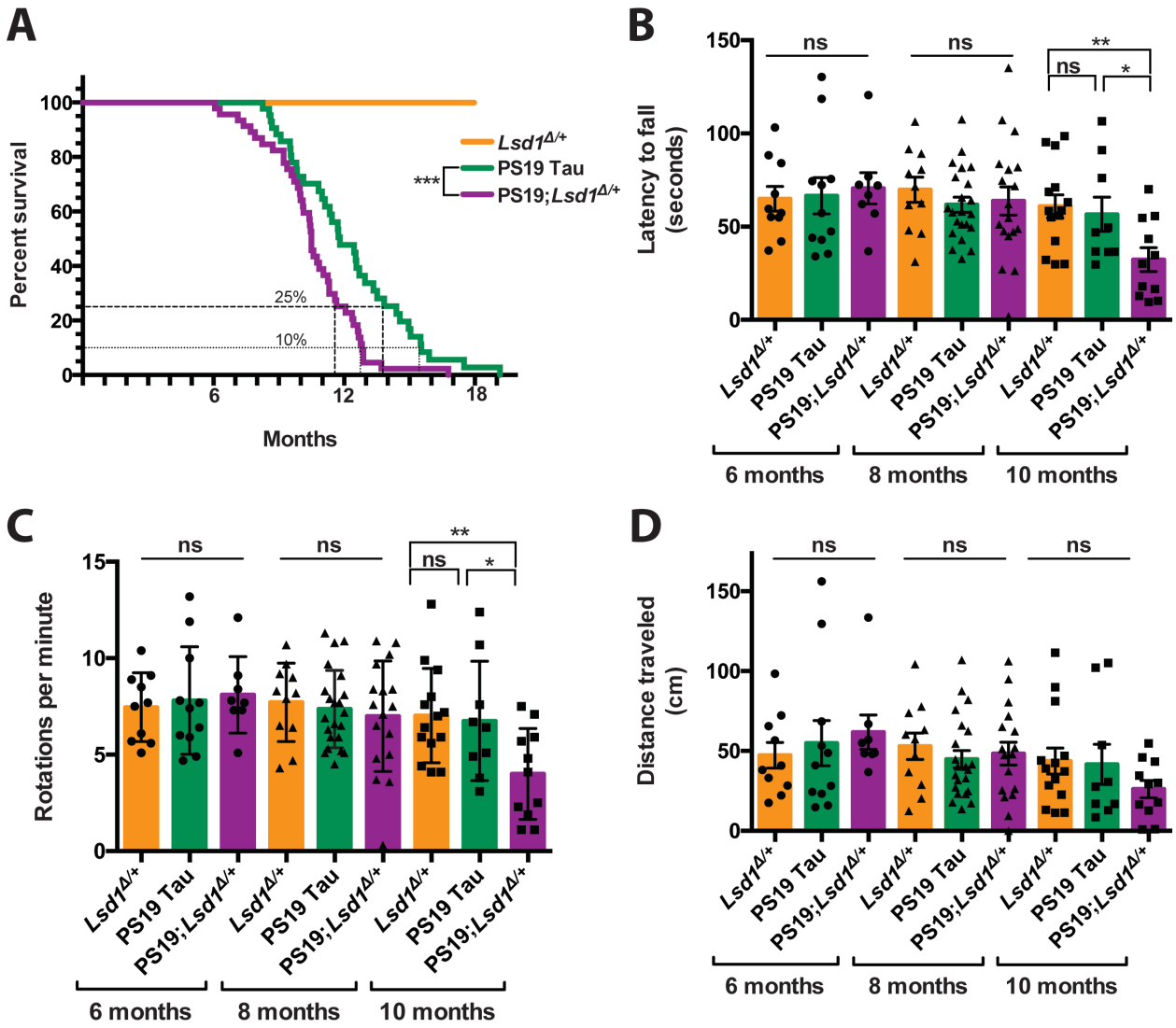

Fig. 2: Reduction of *Lsd1* exacerbates the PS19 Tau mouse paralysis phenotype. A, Lifespan curve showing that no *Lsd1*$^{\Delta/+}$ mice died before 18 months (orange, *n*=20). PS19;*Lsd1*$^{\Delta/+}$ mice (purple, *n*=44) have a significant reduction in survival compared to PS19 Tau mice with wild-type levels of *Lsd1* (green, *n*=37)(Log-rank Mantle-Cox test ***P<0.005). **B-D**, Rotarod testing of latency to fall (in seconds) (**B**), rotations per minute (when the mouse fell) (**C**), and distance traveled (in centimeters) (**D**) for mice at age 6, 8 and 10 months. *Lsd1*$^{\Delta/+}$ (orange, *n*=10,11,14), PS19 Tau (green, *n*=11,22,9), and PS19;*Lsd1*$^{\Delta/+}$ (purple, *n*=8,17,11). Values are mean ± SEM (two-way analysis of variance (ANOVA) with Tukey's post hoc test *P<0.05 **P<0.01, ns=not significant).

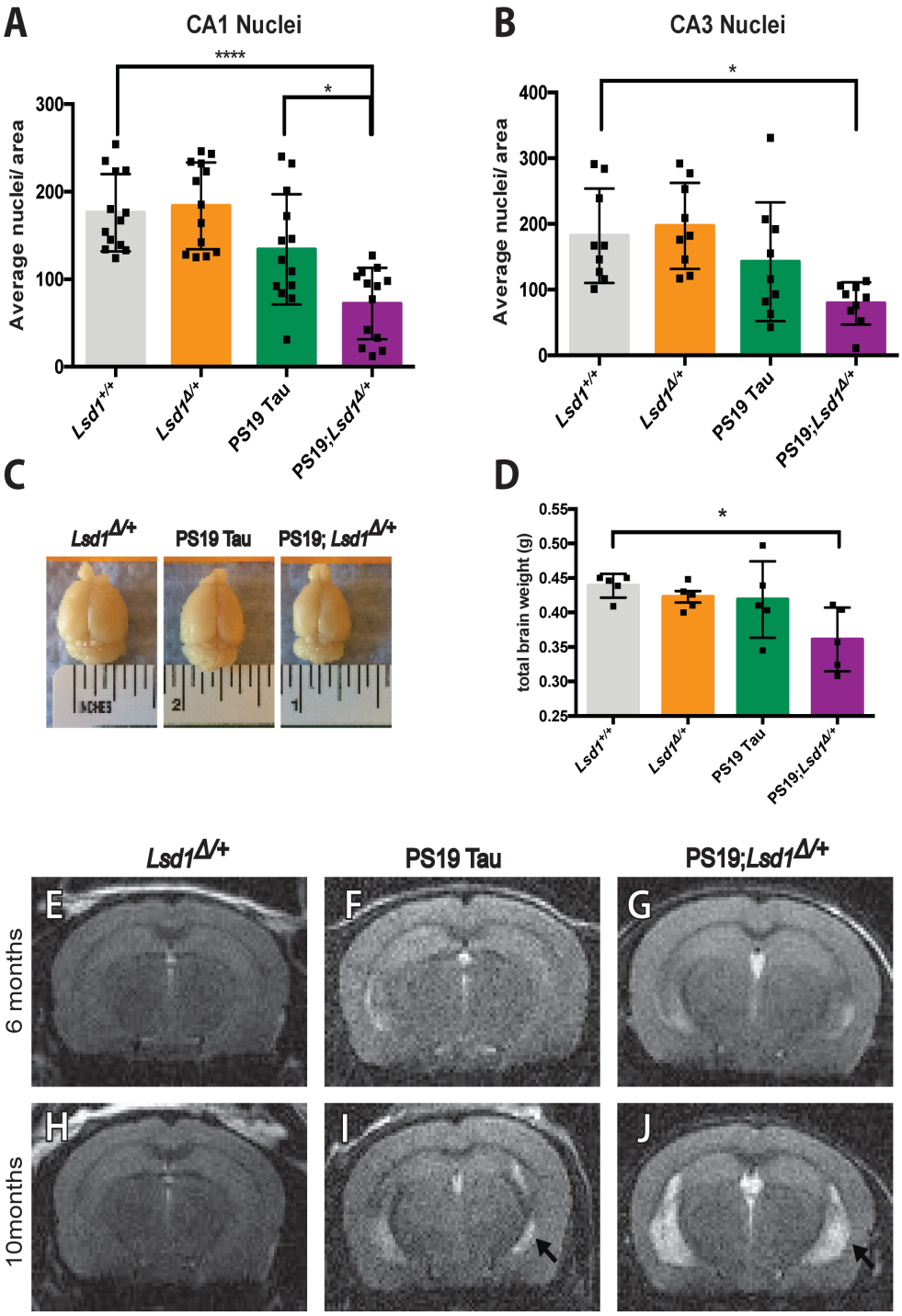

Fig. 3: Reduction of *Lsd1* exacerbates neurodegeneration in PS19 Tau mice. A,B, Average nuclei per area in the CA1 (**A**) and CA3 (**B**) regions of the hippocampus in 12 month old *Lsd1*$^{+/+}$, *Lsd1*$^{\Delta/+}$, PS19 Tau, and PS19;*Lsd1*$^{\Delta/+}$ mice. Quantification from histology represented in **Fig. S5 A-H**. Values are mean ± SD (**A**, *n*=13 & **B,** *n*=9). **C,** Representative image of the brains of 12 month old *Lsd1*$^{\Delta/+}$, PS19 Tau, and PS19;*Lsd1*$^{\Delta/+}$ littermates. **D,** Total brain weight of 12 month old littermates represented in **Fig. 3C.** Values are mean ± SD (*n*=5). For all graphs: one-way analysis of variance (ANOVA) with Tukey's post hoc test (two-sided) *P<0.05,****P<0.001. **E-J,** Representative image of T2- weighted RARE coronal MRI taken from 6 months (**E-G**) and 10 months (**H-jJ**) of age in *Lsd1*$^{\Delta/+}$ (**E,H**), PS19 (**F,J**), and PS19;*Lsd1*$^{\Delta/+}$ (**G,J**) mice (*n*=3). Arrow denotes region of hippocampal atrophy.

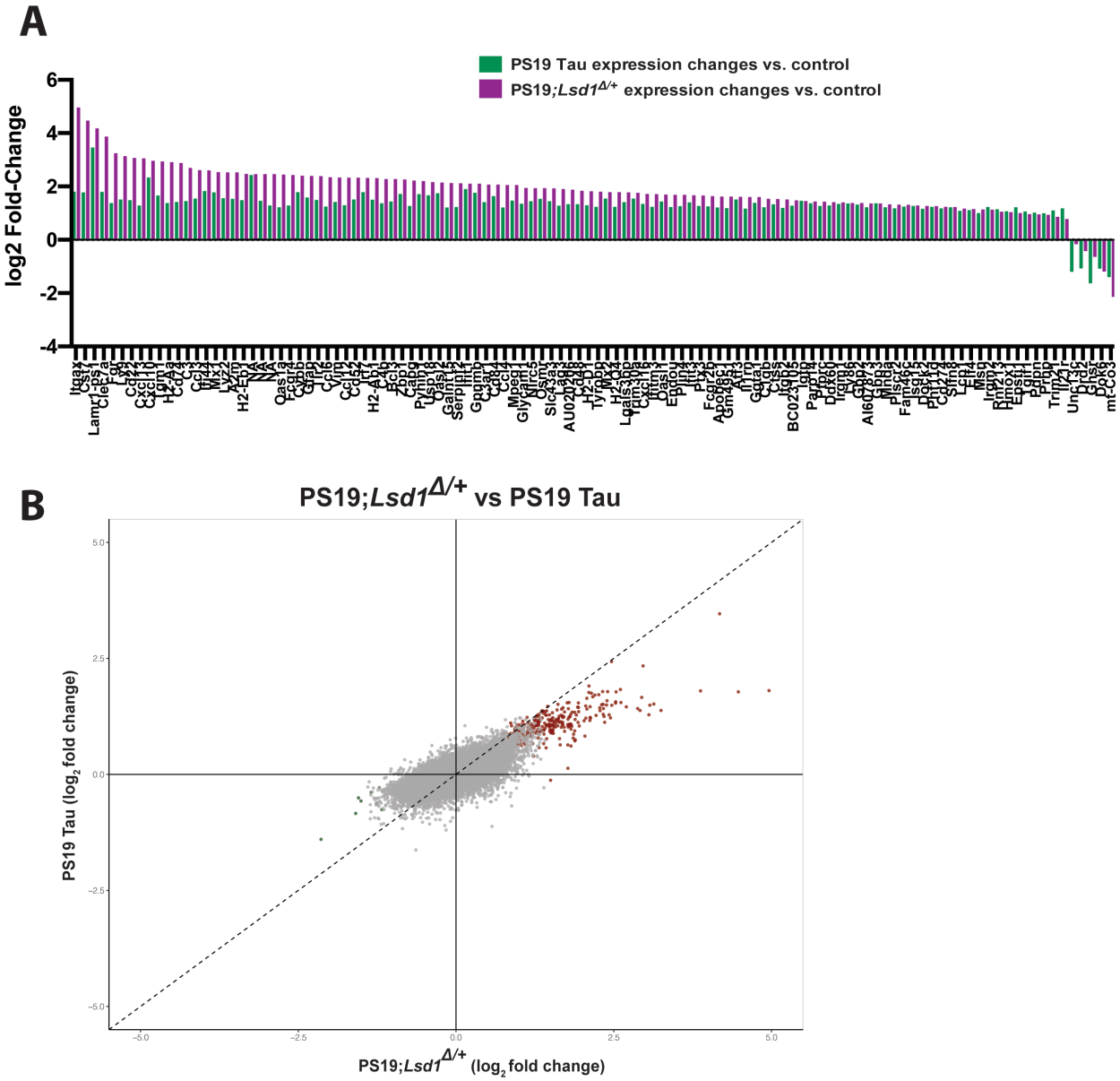

Fig. 4: Molecular overlap between loss of LSD1 function and tauopathy. A, Histogram ($\log_2$ fold change) of the 112 genes that have significant changes in gene expression in the PS19 Tau mice (green, *n*=4) and their corresponding gene expression change in PS19;*Lsd1*$^{\Delta/+}$ mice (purple, *n=4*). **B,** Scatter plot showing the correlation between the genome-wide $\log_2$ fold change in gene expression between PS19 Tau and PS19;*Lsd1*$^{\Delta/+}$. The most significantly changed genes in PS19;*Lsd1*$^{\Delta/+}$ mice are shown in red (upregulated) and green (downregulated). All other genes are shown in grey. Dotted line represents 1:1 relationship between gene expression changes in PS19 Tau vs. PS19;*Lsd1*$^{\Delta/+}$. Exacerbated genes fall to the right of the dotted line in the positively correlated quadrant and to the left of the dotted line in the negatively correlated quadrant. Genes with correlated expression changes are found in the top right and bottom left quadrants, while genes that do not correlate are found in the opposite quadrants.

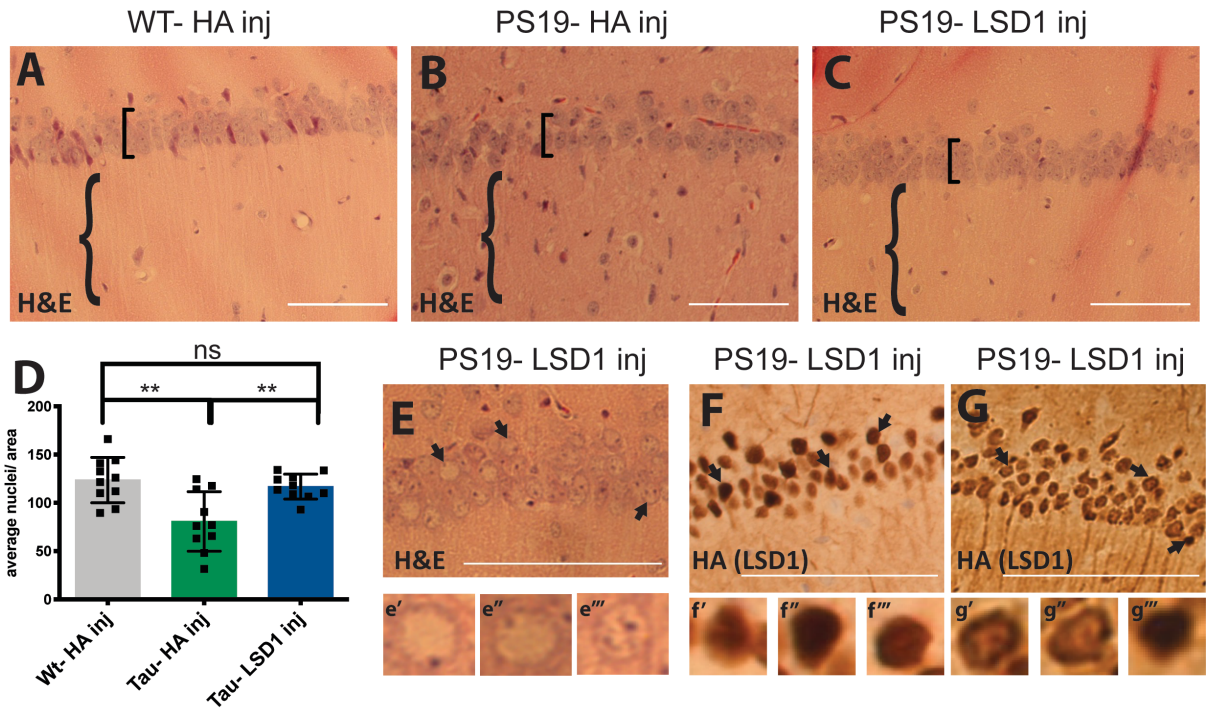

Fig. 5: LSD1 overexpression rescues the neurodegenerative phenotype in the hippocampus of 11 month old PS19 Tau mice. A-C, Representative image of H&E stained CA1 region of the hippocampus of 11 month old Wild Type mice injected with HA control virus (WT- HA inj) (**A**), PS19 Tau mice injected with HA control virus (PS19-HA inj) (**B**), and PS19 Tau mice injected with *Lsd1* overexpressing virus (PS19- LSD1 inj) (**C**). Square brackets denote thickness of pyramidal layer of the CA1 of the hippocampus and curvy brackets denote hippocampal region with or without infiltrating cells. **D,** Quantification of the average number of nuclei in the pyramidal layer of the hippocampus per area per mouse from histology represented in **Fig. 5A-C**. Values are mean ± SD (*n*=10, one-way analysis of variance (ANOVA) with Tukey's post hoc test, **p<0.01, ns=not significant). **E,** Representative H&E of PS19- LSD1 inj mouse with abnormal nuclei blebbing in the CA1 region of the hippocampus. **E'-E''',** High magnified image of cells denoted by arrows in **Fig. 5E** of individual nuclei that are either abnormally blebbed (**E', E"**) or normal (**E'''**). **F,G,** Immunohistochemistry staining of HA(LSD1) in 11 month PS19- LSD1 inj mice. HA is either localized specifically to the nucleus in all nuclei (**F**) or in only a few nuclei while it is partially sequestered in the cytoplasm in others (**G**). **F'-F''',** High magnified image of cells denoted by arrows in **Fig. 5F** of nuclear HA localization in individual nuclei. **G'-G''',** High magnified image of cells denoted by arrows in **Fig. 5G** of individual nuclei with HA(LSD1) either sequestered to the cytoplasm (**G', G"**) or confined to the nucleus (**G'''**). Scale bars=50µm.

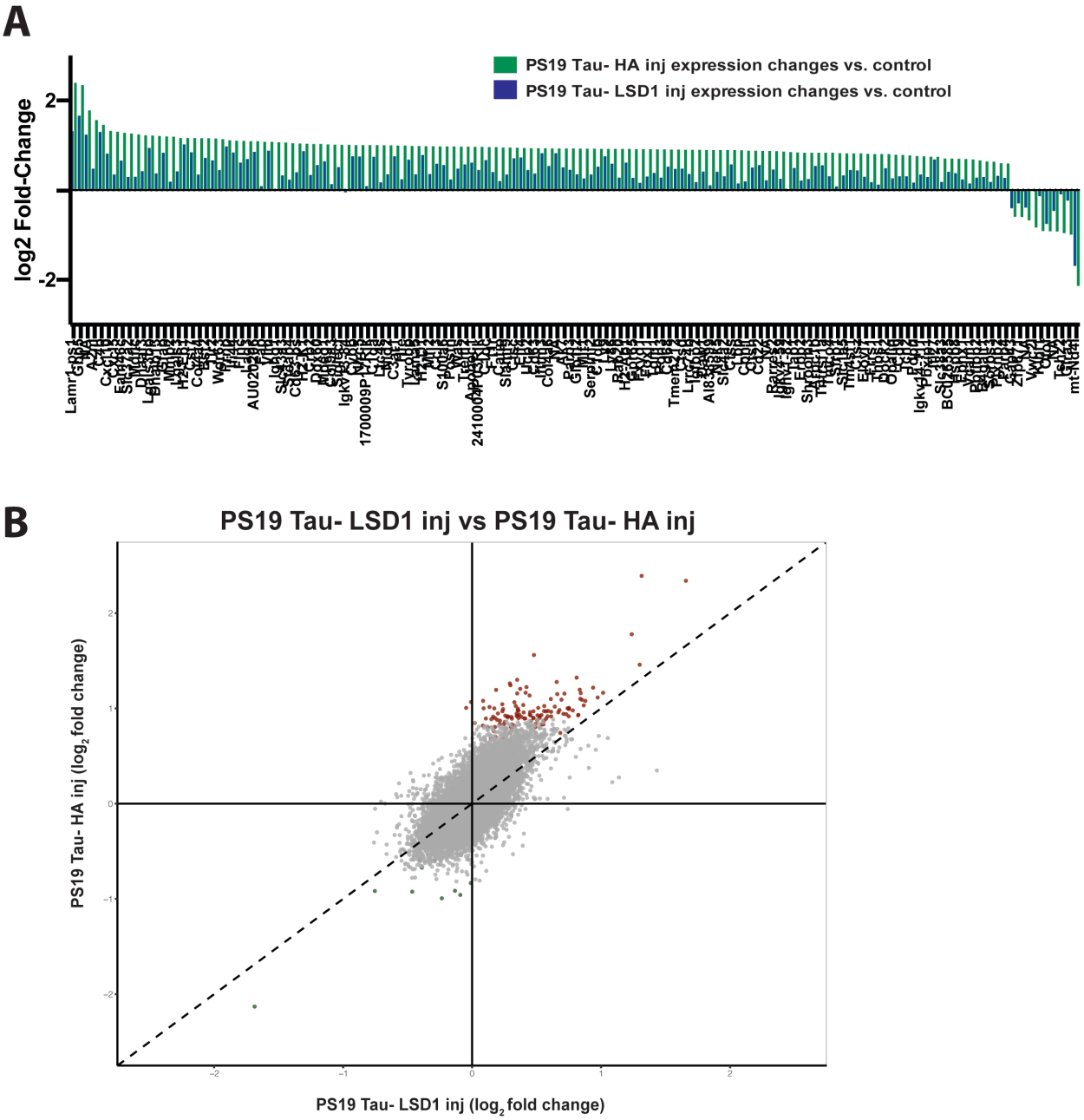

Fig. 6: Molecular overlap between loss of LSD1 function and tauopathy. A, Histogram ($\log_2$ fold change) of the 144 genes that have significant changes in expression in the PS19 Tau- HA inj mice (green, n=3) and their corresponding gene expression changes in the PS19 Tau- LSD1 inj mice (blue, n=3). **B,** Scatter plot showing the correlation between the genome-wide $\log_2$ fold change in gene expression between PS19 Tau- HA inj and PS19 Tau- LSD1 inj. The most significantly changed genes in the PS19 Tau- HA inj mice are shown in red (upregulated) and green (downregulated). All other genes are shown in grey. Dotted line represents 1:1 relationship between gene expression changes in PS19 Tau- Ha inj and PS19 Tau- LSD1 inj. Rescued genes fall to the left of the dotted line in the positively correlated quadrant and to the right of the dotted line in the negatively correlated quadrant. Genes with correlated expression changes are found in the top right and bottom left quadrants, while genes that do not correlate are found in the opposite quadrants.